



Single walled carbon nanotube anodes based high performance organic light-emitting diodes with enhanced contrast ratio

Feng Xu ^{a,b}, Wen Qing Zhu ^{a,b,*}, Long Yan ^c, Hong Xu ^{a,b}, Ling Hao Xiong ^{a,b}, Jia Heng Li ^{a,b}

^a School of Material Science and Engineering, Shanghai University, Shanghai 200072, China

^b Key Laboratory of Advanced Display and System Applications, Ministry of Education, Shanghai University, Shanghai 200072, China

^c Shanghai Institute of Applied Physics, Chinese Academy of Science, Shanghai 201800, China

ARTICLE INFO

Article history:

Received 5 September 2011

Received in revised form 18 November 2011

Accepted 20 November 2011

Available online 14 December 2011

Keywords:

Single walled carbon nanotubes (SWCNTs)

Organic light-emitting diodes (OLEDs)

SWCNT anode

Contrast ratio

ABSTRACT

Commercially-available single walled carbon nanotubes (SWCNTs) were used to fabricate SWCNT sheets for anodes of organic light-emitting diodes (OLEDs) by spray-coating process without any use of surfactant or acid treatment. A layer of DMSO doped PEDOT:PSS was spray-coated on the SWCNT sheets to not only lessen the surface roughness to an acceptable level, but also improve the conductivity by more than three orders of magnitude. For our SWCNT-based OLEDs of tris-(8-hydroxyquinoline) aluminum (Alq₃) emission layers, a maximum luminance 4224 cd/m² and current efficiency 3.12 cd/A were achieved, which is close to the efficiency of ITO-based OLEDs. We further found out that our OLEDs based on the PEDOT:PSS covered SWCNT anodes tripled the contrast ratio of the conventional indium tin oxide (ITO) based OLEDs.

© 2011 Elsevier B.V. All rights reserved.

1. Introduction

Over the past decade, enormous efforts have been made to fabricate highly conductive, transparent, flat and flexible single-wall carbon nanotube (SWCNT) sheets for their potential to substitute and surpass the conventional transparent conducting oxide—indium tin oxide (ITO) in an extensive variety of optoelectronic devices [1–5]. For ITO suffers from the drawbacks of high cost, inherent brittleness, and need for high-temperature processing [6,7], it is not an ideal choice for large-area and flexible application. As transparent anode material for organic light-emitting diodes (OLEDs), SWCNT has a work function (of 4.5–5.1 eV) [8] similar to or even better than that of ITO (4.4–4.9 eV) [9]. In addition, the SWCNT sheet boasts key properties such as flexibility, transparency, high conductivity and fitness of solution process, which is a promising candidate to replace ITO in OLED technology for flexible applications and mass-manufacture.

Several groups have reported SWCNT sheets parallel to ITO sheets with low sheet resistance below 200 Ω/sq accompanying high transmittance above 80% in visible region, using surfactant and acid treatment [3,10–14].

However, the OLEDs based on these SWCNT sheets had hardly acquired the satisfactory performance as the ITO-based OLEDs did [3,13,15]. Besides the attribution that the inherent excessive surface roughness of SWCNT sheets due to SWCNT's large aspect ratio should be responsible for the difference between SWCNT based and ITO based OLEDs, during the process of fabricating these SWCNT sheets, it is found that although some surfactants can result in stable dispersion by structureless random absorption on SWCNTs [16], they also cover up and denature the SWCNTs [17,18] in addition to more or less the toxicity they have. Moreover, the subsequent acid treatment has been reported to destroy most SWCNTs [19–21], poison the emissive layer for the presence of residual mobile counterions and can cause delamination from the underlying substrate, affecting the properties of devices based on these SWCNTs.

In this paper, we report a high performance OLED based on the SWCNT anode, which achieved a maximum luminance and current efficiency of 4224 cd/m² and 3.12 cd/A,

* Corresponding author at: School of Material Science and Engineering, Shanghai University, Shanghai 200072, China. Tel./fax: +86 021 56334387.

E-mail address: wqzhu@shu.edu.cn (W.Q. Zhu).

respectively. The commercially-available SWCNTs were used to fabricate SWCNT sheets by spray-coating process with no use of any surfactant or acid treatment. Dimethyl sulfoxide (DMSO) doped poly(3,4-ethylenedioxythiophene): poly(styrenesulfonate) (PEDOT:PSS) [22] was used to improve the resistance and surface roughness of SWCNT sheets. Finally, the optical properties of the SWCNT anode based OLEDs were explored. The result demonstrated a triple contrast ratio higher than that of the conventional ITO-based OLEDs.

2. Materials and methods

The SWCNTs were purchased from Shenzhen Nanotech Port Co. Ltd. with CNT purity >90 wt.%, SWCNT purity >60 wt.%, outer diameter <2 nm and length in the range of 5–15 μm . The SWCNT sheets were fabricated by spray-coating process suitable for adjusting the sheet resistance and transmittance from 0% to 100% [4]. We started by dispersing the SWCNTs in ethanol solvent with the aid of ultrasonic treatment, and then the homogeneous dispersion (of 0.25 mg/ml SWCNTs) without further purification was spray-coated on the heated glass substrate at 120 $^{\circ}\text{C}$, followed by 3-h drying at 85 $^{\circ}\text{C}$. Through a patterned shadow mask, two SWCNT sheets were spray-coated on a glass substrate. On each of the four edges of the glass substrate, two rectangular ITO thin films were sputtered, acting as connecting electrodes to SWCNT sheets or to Aluminum electrodes. The inset image in Fig. 1 shows two SWCNT sheets with dimension of 5 \times 25 mm spray-coated on the glass substrate.

In order to improve the conductivity and solve the problems like short-circuit or nonuniform injection of holes caused by the excessive surface roughness of SWCNT sheets, a 150 nm, 60 Ω/sq with 83.1% transmittance (at $\lambda = 538 \text{ nm}$) planarization layer of PEDPT:PSS was directly

spray-coated on the SWCNTs sheets. A concentration of 5 wt% DMSO was added continuously into the solution of PEDOT:PSS (BAYTRON[®] PH500) while being stirred, by which an improvement in conductivity of more than three orders of magnitude could be achieved [23]. Previously, the planarization layer was commonly spin-coated on the SWCNT sheet's surface [3,13–15,24]. Considering that the uniformity and morphology of SWCNT sheets spray-coated on the glass substrate may be degraded by spin-coating process, where the spin-coated solution is dipped on the surface of SWCNT sheets, and to some extent, disperses the SWCNT sheet, resulting in the degradation of the form and structure of it, we spray-coated the PEDOT:PSS solution on the SWCNT sheets at 110 $^{\circ}\text{C}$, after mixing one PEDOT:PSS solution with nine ethanol followed by 30-min ultrasound. Finally, the PEDOT:PSS covered SWCNT sheets were put into the drying oven at 80 $^{\circ}\text{C}$ for three hours.

The OLEDs were eventually completed using a stake of small molecular organic layers and metal cathode in multisource organic molecular vapor deposition system at $3.0 \times 10^{-4} \text{ Pa}$. The organic stack consists of 50 nm *N,N*-diphenyl-1,1-bihyl-4,4-diamine(NPB) and 60 nm tris-(8-hydroxyquinoline) aluminum (Alq_3). The cathode layer consists of 0.5 nm lithium fluoride (LiF) and 100 nm aluminum on the organic layer deposition. On one piece of glass substrate, 4 diodes were fabricated with dimension of 5 \times 5 mm for each. Fig. 2(c) and (d) show the schematic diagram of the device structure and the photograph of an operating SWCNT-based OLED device.

The transmittance of the SWCNT sheets was obtained from the ratio of the measured transmittance of SWCNTs-coated glass, by MODEL U-3900H Spectrophotometer, to that of the glass substrate prior to spray-coating. The sheet resistance was measured by a four point method with CT5601Y Sheet Resistivity Meter. The AFM images and the

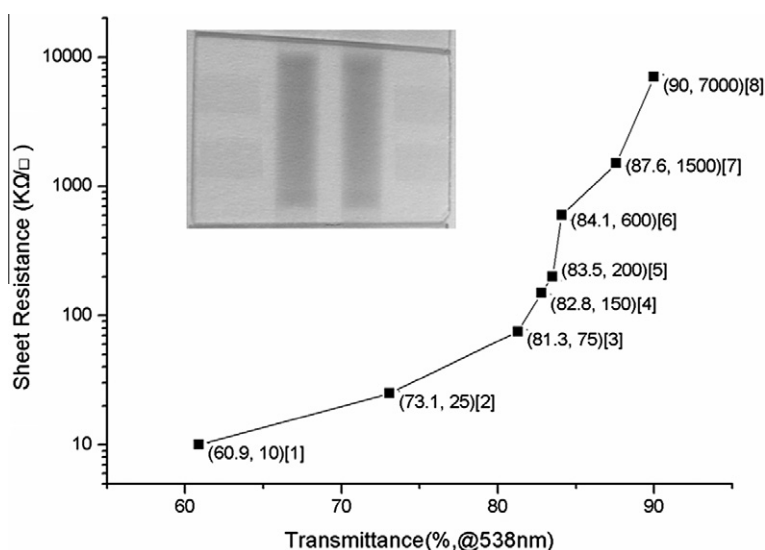


Fig. 1. The sheet resistance of spray-coated SWCNT sheets as a function of the transmittance at a wavelength of 538 nm (corresponding to the peak emission of OLEDs in our experiments). The inset image is the photograph of spray-coated SWCNT sheets on a glass substrate.

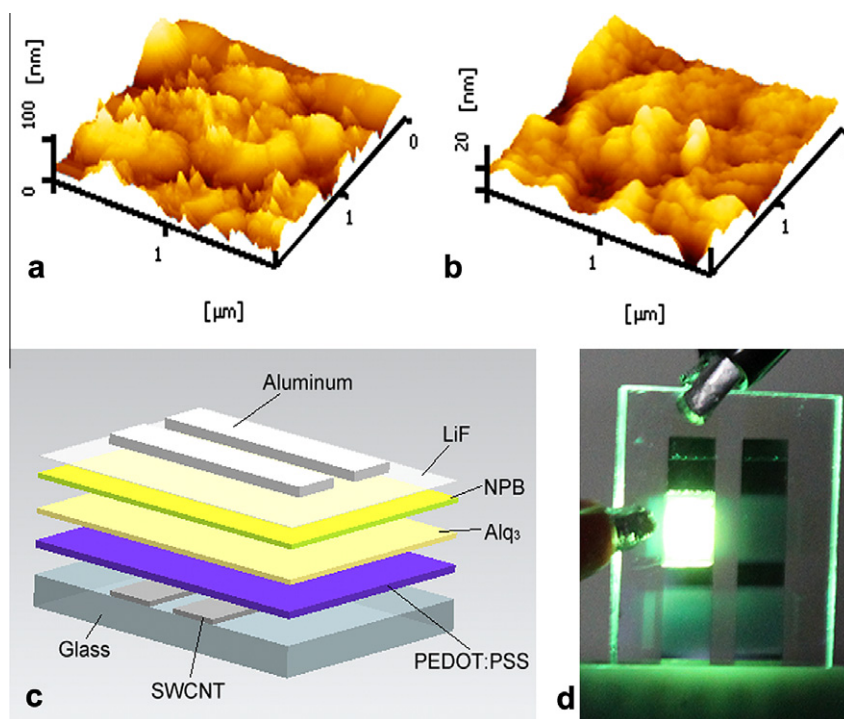


Fig. 2. (a) AFM image of a spray-coated SWCNT sheet, (b) AFM image of a PEDOT:PSS modified SWCNT sheet, (c) schematic diagram of the OLED device based on the SWCNT anode, (d) the photograph of an operating SWCNT anode based OLED device.

roughness data were obtained through AFM Nanonavi SPA-400 SPM. The OLEDs measurement of current–voltage relationship and the electroluminescent spectra was carried out using Keithly source meter 2400 and Spectra Scan PR650. The reflectance spectra of the OLED devices were taken on a MODEL U-3900H Spectrophotometer.

3. Results and discussion

Firstly, we investigated the issues about the SWCNT anodes fabricated by spray-coating process. Compared with ITO sheets displaying both high transmittance (>80%) and low resistance ($\sim 20 \Omega/\text{sq}$) [25], our SWCNT sheets' connection between transmittance and sheet resistance is comparatively inferior. As shown in Fig. 1, the sheet resistances of spray-coated SWCNT sheets increased from 10 to 7000 $\text{k}\Omega/\text{sq}$ while their transmittances ascended from 60% to 90%. These series of sheet resistance are over one order of magnitude more than the SWCNT sheets made by filtration method published by Wu et al. [10]. Two main reasons contribute to this high sheet resistance: one is the presence of resistive impurities in the commercially-available SWCNT powder, and the absence of surfactant or any acid treatment in the SWCNT dispersion process; the other is the difference of SWCNT forming process. In a spray-coated SWCNT sheet, randomly accumulate the carbon nanotubes in both vertical and horizontal directions. But in the filtration and transfer process, the carbon nanotubes tend to lie horizontally on the filtration membrane under

the influence of liquid flow and on the substrate after transfer printing. The horizontal helps the in-plane conductivity more; the vertical contributes that in the z-axis direction more. That probably explains why the spray-coated or airbrushed SWCNT sheets [4,5,26,27] always show higher sheet resistance and roughness than filtrated SWCNT sheets [3,10,15,28] do.

Through spray-coating PEDOT:PSS planarization layer, the sheet resistance and surface roughness of the SWCNT sheets acquired significant improvements. In Table 1, a comparison of the sheet resistances and transmittance of SWCNT sheets before and after spray-coating PEDOT:PSS layer reflects an obvious plunge in sheet resistance. Eight samples were divided into two groups, samples from 1 to 4 as group I and samples from 5 to 8 as group II. View the series of changed sheet resistances in group I and group II separately from each other, a monotonous increase is clear going along with the adding of original sheet resistances. What unexpected is that the series of sheet resistances in group II after spray-coating planarization layer plunged even further, much lower than those of the samples in group I which had the lower original sheet resistances of SWCNTs. It is probably because when SWCNT sheet resistance is so high as to approach $200 \text{ k}\Omega/\text{sq}$, on the glass substrate disperses the SWCNTs relatively scatteredly and the spraying of the PEDOT:PSS could easily fill into the gaps in the SWCNT sheets, forming a high conductivity composite layer which significantly improves the resistance. Meanwhile, the internal SWCNTs increased the conductive paths in the PEDOT:PSS layer. That is why

Table 1

Sheet resistance (R_{sq}) and transmittance (T%) variation before and after spray-coating of PEDOT:PSS.

Sample ID	Original R_{sq} and T% ($k\Omega/sq, \%$)	Modified R_{sq} and T% ($k\Omega/sq, \%$)
1	(10, 60.9)	(0.5, 44.5)
2	(25, 73.1)	(1.0, 57.3)
3	(75, 81.3)	(1.2, 63.7)
4	(150, 82.8)	(1.5, 64.3)
5	(200, 83.5)	(0.03, 64.1)
6	(600, 84.1)	(0.03, 66.5)
7	(1500, 87.6)	(0.04, 69.7)
8	(7000, 90.0)	(0.05, 73.2)

these samples in group II exhibited even lower sheet resistance than PEDOT:PSS layer itself ($60 \Omega/sq$). Similarly, this mutual-benefit effect has been previously reported by J.N. Coleman group [29]. They found that the electrical/optical properties of these composites from SWCNT blended with PEDOT:PSS were actually superior to the nanotube-only films. We noted that the optimal OLED device was gained when based on the SWCNT sheet anode of 83.5% transmittance accompanying $200 k\Omega/sq$ sheet resistance, which turned into 64.1% and $30 \Omega/sq$ respectively after spray-coating of PEDOT:PSS. The OLED device's performance is

discussed in the later part of this paper. The transmittance's behavior after the spray-coating, not that complicated, showed a 15–20% decline off the original.

Besides the improvement on sheet resistance, spray-coated PEDOT:PSS layer demonstrated the same effect on addressing the surface roughness of SWCNT sheets as the spin-coated did. Fig. 2 shows a comparison between AFM image (a) and (b), illustrating the morphological amendment after spray-coating a PEDOT:PSS layer. At first, the average surface roughness of the $200 k\Omega/sq$ SWCNT sheet was around 15.5 nm rms, which is high enough to induce a device failure for any OLED of which the integrated thickness is within the range of 200 nm. After spray-coating directly a 150 nm PEDOT:PSS layer on the SWCNT sheets, the surface roughness was substantially reduced to 4.2 nm, quite close to 2.4 nm of ITO films.

Next we discuss the electroluminescent performance of OLEDs with different anodes, ITO, PEDOT:PSS and SWCNTs with planarization layer of PEDOT:PSS. Fig. 3 shows the performance comparison among these OLEDs. We had tried as well OLED devices based on SWCNT sheet anodes without planarization layers, but its luminance was very low and the device failed too quickly to allow enough time for any characterization. The OLED based on the polymer anode, PEDOT:PSS, was fabricated to have a comparison

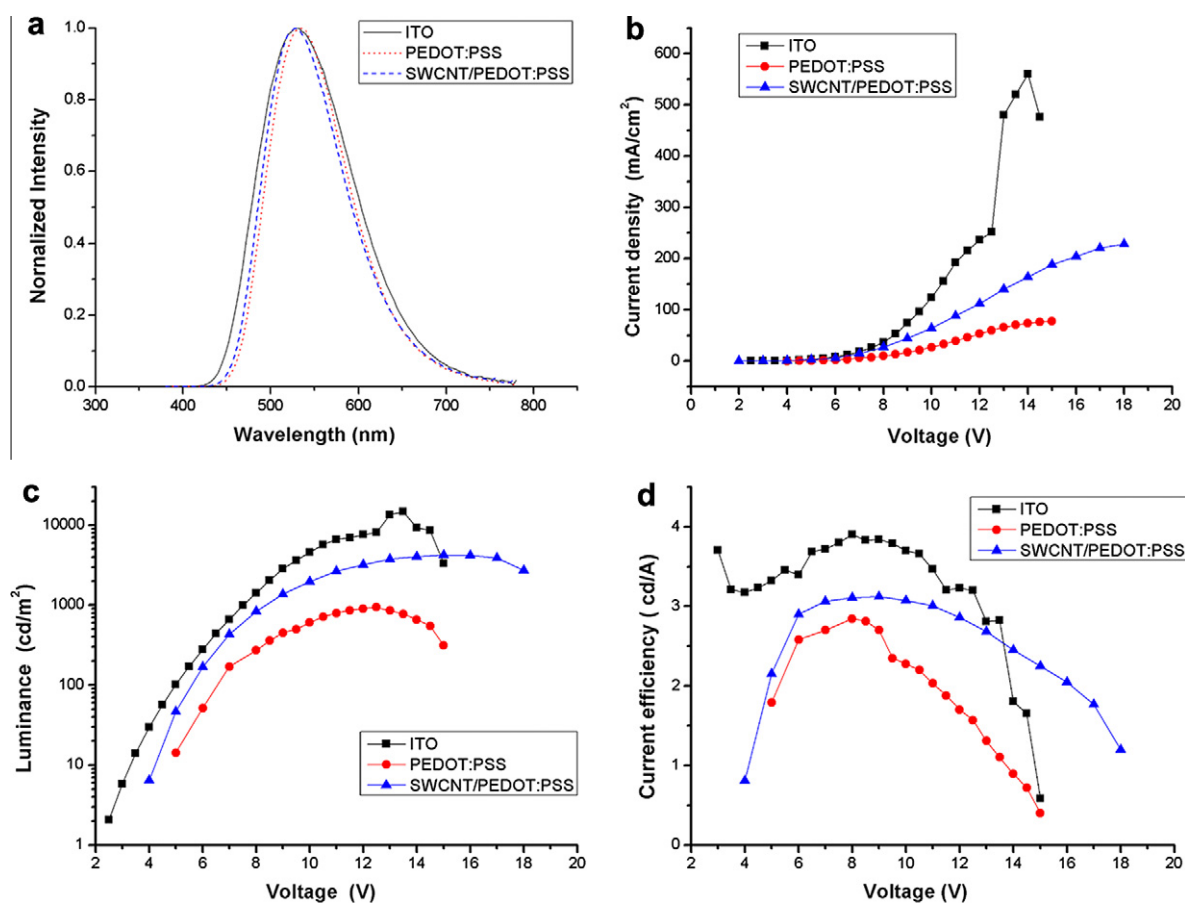


Fig. 3. Electroluminescent characteristics of OLED devices based on diverse anodes, ITO, PEDOT:PSS and SWCNTs covered by PEDOT:PSS, (a) normalized electroluminescence spectra, (b) current density vs voltage, (c) luminance vs voltage, (d) current efficiency vs voltage.

with that based on the SWCNT sheet covered by PEDOT:PSS planarization layer. Among all SWCNT sheet samples, the one having the lowest sheet resistance after spray-coating PEDOT:PSS layer turned out to produce the best electroluminescent performance. That was the 200 k Ω /sq SWCNT sheet, which turned into 30 Ω /sq after spray-coating PEDOT:PSS layer.

Modifying the SWCNT sheet by spray-coating PEDOT:PSS planarization layer on it enabled the OLED an substantial improvement on stability and electroluminescent performance, which should be ascribed to the amendment of surface roughness from 15.5 to 4.2 nm and the plunge of sheet resistance from 200 to 30 Ω /sq. The achieved maximum luminance was 4224 cd/m² at 15 v, and current efficiency peaked at 3.12 cd/A when bias was 9 v. This performance surpassed all the other having been reported SWCNT anode OLED devices with Alq₃ as light-emitting material, and seemed the closest to that of the conventional ITO-anode OLEDs. T. Mark group had also reported their polymer OLED devices (with a superior light-emitting layer, TFB + BT [30]) based on the SWCNT anode and spin-coated PEDOT:PSS planarization layer [14,31]. However, in that case, the optimal device achieved a maximum light output of 3500 cd/m² and a current efficiency of 1.6 cd/A. The higher luminance and efficiency achieved in our Alq₃ light-emitting material OLED should be attributed to the highly conductivity and spray-coating process of PEDOT:PSS planarization layer in addition to the absence of negative effects caused by the use of surfactant and acid treatment. 5 wt% DMSO doped into the PEDOT:PSS composition considerably decreased the sheet resistance of the planarization layer to 60 Ω /sq; The spray-coating process avoided not only the poor interfacial contact problem existing in the spin-coating process between the PEDOT:PSS layer and the SWCNT sheet, which inherently possesses the hydrophobic nature, but also damaging the uniformity and morphology of SWCNT sheets, which happens more or less in the spin-coating process. These factors lead to the higher brightness and current efficiency as well as uniform light output of our SWCNT anodes based OLED devices.

What's more, it is also distinct from the Fig. 4 that SWCNT sheets incorporating a planarization layer of spray-coated PEDOT:PSS resulted in better device performance than individual PEDOT:PSS functioning as OLED anodes did. The OLEDs based on PEDOT:PSS anode showed a maximum luminance around 1000 cd/m² at 12.5 V and current efficiency of 2.85 cd/A. The better performance would be due to the lower sheet resistance of the PEDOT:PSS-modified SWCNT anode of 30 Ω /sq over the PEDOT:PSS sheet of 60 Ω /sq, as well as the improvement on the stability and electrical inhomogeneity of PEDOT:PSS by the presence of SWCNT conductive paths in it. The ITO-based OLED behaved best among the three mainly due to its smooth surface (2.4 nm rms), low sheet resistance 12 Ω /sq putting together with high transmittance of around 90% within the visible region. In addition, we noted, from Fig. 3(a), that the incorporation of PEDOT:PSS polymer as either the anode or the planarization layer brought no shift to the electroluminescent spectra of OLED devices despite the fact that PEDOT:PSS layer of 150 nm thickness was light blue itself.

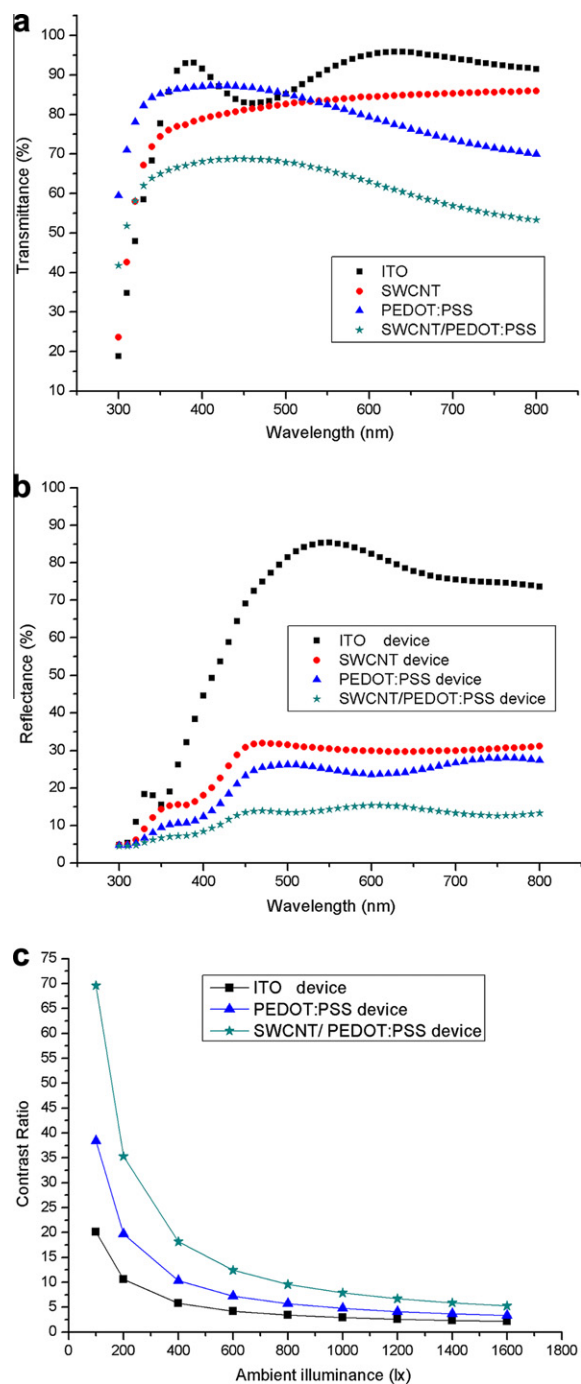


Fig. 4. (a) The transmittance from 300 to 800 nm of the 12 Ω /sq ITO, the 200 K Ω /sq SWCNT, the 60 Ω /sq PEDOT:PSS as well as the 30 Ω /sq PEDOT:PSS covered SWCNT anodes, (The glass substrate was set to be the baseline.) (b) Measured spectral reflectance from 300 to 800 nm of OLED devices based on the ITO anode, the SWCNT anode, the PEDOT:PSS anode and the PEDOT:PSS covered SWCNT anode, (c) Contrast ratio as a function of ambient illuminance from 100 to 1600 lx of OLED devices based on various anodes. The contrast ratio was calculated using $L_{on} = 300$ cd/m² and $L_{off} = 0$ cd/m².

Finally, we explored the effects of SWCNT anodes on the optical properties of OLEDs. Fig. 4(a) shows the transmittance comparison of various anodes. They are the 12 Ω /sq ITO, the 200 K Ω /sq SWCNT, the 60 Ω /sq PEDOT:PSS sheet as well as the 30 Ω /sq PEDOT:PSS covered SWCNT sheet. Both the SWCNT sheet and the PEDOT:PSS sheet exhibited a \sim 80% transmittance from 300 to 800 nm. When piled together, they exhibited an integrated transmittance about 60%. And we further found that the comparatively low transmittance of PEDOT:PSS covered SWCNT anode paid off in the aspect of high contrast ratio.

The pixel contrast ratio (PCR) of the OLED was calculated by using the equation [32]:

$$\text{PCR} = \frac{L_{\text{on}} + R_L L_{\text{ambient}}}{L_{\text{off}} + R_L L_{\text{ambient}}} \quad (1)$$

where L_{on} and L_{off} are the luminance of a pixel at “on” and “off” states respectively, L_{ambient} is the ambient illumination, and R_L is the luminous reflectance, which can be expressed as:

$$R_L = \frac{\int_{\lambda_1}^{\lambda_2} V(\lambda) S(\lambda) R(\lambda) d(\lambda)}{\int_{\lambda_1}^{\lambda_2} V(\lambda) S(\lambda) d(\lambda)} \quad (2)$$

The Luminous reflectance is defined as the normalized integrated product of $V(\lambda) \cdot S(\lambda) \cdot R(\lambda)$, where $V(\lambda)$ is the standard photonic curve, $S(\lambda)$ is the spectrum of Alq₃ in our experiment, and $R(\lambda)$ is the spectral reflectance of the device. The measurement was carried out from wavelength $\lambda_1 = 300$ nm to $\lambda_2 = 800$ nm.

From Eq. (1), we can easily comprehend that under low ambient light levels, the PCR is given approximately by the luminance ratio of the on pixel to the off pixel; under high illumination levels, the contrast ratio deteriorates and the display image can be washed out unless the on pixel has an extremely high luminance or the luminous reflectance is very low. However, increasing the luminance of the pixels to compensate for the high ambient light levels can lead to a shorter lifetime for display and reliability problems. Therefore, recently many approaches have been proposed to reduce the luminous reflectance R_L by using an optical interference layer, a semitransparent cathode, a light absorbing layer and a phase-changing layer. Hung and Madathil fabricated an OLED device with a reflection-reducing layer of zinc oxide, which markedly reduces the ambient light reflected from the cathode [33]. Xie and Hung developed a high contrast OLED device with a low-reflection cathode by depositing a multilayer structure over semitransparent cathode of Sm [34]. Li et al. demonstrated an OLED device with a high contrast ratio, made of copper phthalocyanine (CuPc) as the black-layer material [35]. The absorption and destructive interference effect of CuPc layer reduced the ambient light. However, the efficiency of the OLED with an inserted anti-reflection layer is half that of a conventional device, since the reflection of light from the metal cathode is reduced.

Fig. 4(b) shows the spectral reflectance of OLED devices with the four different anodes. The conventional ITO anode OLED had an average spectral reflectance as high as around 80% within the range from 300 to 800 nm wavelength. In contrast, the SWCNT anode modified by spray-coated

PEDOT:PSS layer lowered the spectral reflectance of the OLED to less than 15%. An explanation to the decline of spectral reflectance is that the PEDOT:PSS covered SWCNT anode functioned as well a light absorbing layer reducing the ambient light injected into the device and the reflection of ambient light from the metal cathode. What different from the reported contrast-enhanced OLED devices [34–36] is that the light absorbing layer is located on the anode position not the cathode side, which preserved the Al cathode's reflective effect on the luminescence of light-emitting layer and hence enhanced light output efficiency.

Taking the measured spectral reflectance $R(\lambda)$ into equation(2) yielded the $R_L = 13.7\%$ of the OLED based on the PEDOT:PSS covered SWCNT anode, which was nearly one-fourth of that of the conventional ITO-based OLED, 49.2%, and one-twice of that of the OLED device based on the PEDOT:PSS polymer anode, 25.5%.

The lower R_L of OLED device can lead to higher contrast ratio of display. Using Eq. (1) and the values of the resultant R_L , we calculated the contrast ratio of the OLED devices based on the various anodes, as presented in Fig. 4(c). It is found that the contrast ratio of OLED based on PEDOT:PSS covered SWCNT anode was over 3 times higher than that of the ITO-based OLED at the ambient illumination from 100 to 1600 lx. The enhancement in the contrast ratio is exactly attributable to the decrease in the luminous reflectance, R_L .

In conclusion, we successfully fabricated high performance OLED devices based on the SWCNT anodes with enhanced contrast ratio. The maximum luminance and current efficiency reached 4224 cd/m² and 3.12 cd/A respectively. By spray-coating process without any use of surfactant or acid treatment, our experiment demonstrated the possibility of using commercially-available SWCNTs and simple process to make OLED device suitable for large-area manufacture. Our work reveals that the spray-coated layer of PEDOT:PSS played a significant role in improving resistance and surface roughness of the SWCNT anode which is critical to the high performance and stability of SWCNT-based OLED devices. We further demonstrated that the OLED device based on PEDOT:PSS covered SWCNT anode exhibited considerably reduced spectral reflectance and enhanced contrast ratio. This can be another advantage of SWCNT over ITO to be employed as transparent anode in the application of OLED displays.

Acknowledgements

The work was supported by National Basic Research Program of China under grant No. 2010CB832903, the National Natural Science Foundation of China (60906019), and supported by Key Project of the Chinese Ministry of Education (209044) as well as the project of Science and Technology Commission of Shanghai Municipality (10dz1140206).

References

- [1] E.S. Snow, J.P. Novak, M.D. Lay, E.H. Houser, F.K. Perkins, P.M. Campbell, Carbon nanotube networks: Nanomaterial for macroelectronic applications, *J. Vac. Sci. Technol. B* 22 (2004) 1990–1994.
- [2] G. Gruner, Carbon nanotube films for transparent and plastic electronics, *J. Mater. Chem.* 16 (2006) 3533–3539.

- [3] Y.Q. Liu, Y. Wang, C.A. Di, H. Kajiura, S.H. Ye, L.C. Cao, D.C. Wei, H.L. Zhang, Y.M. Li, K. Noda, Optimizing Single-Walled Carbon Nanotube Films for Applications in Electroluminescent Devices, *Adv. Mater.* 20 (2008) 4442–4449.
- [4] M. Kaempgen, G.S. Duesberg, S. Roth, Transparent carbon nanotube coatings, *Appl. Surf. Sci.* 252 (2005) 425–429.
- [5] D.W. Kim, S. Paul, Preparation and characterization of highly conductive transparent films with single-walled carbon nanotubes for flexible display applications, *Carbon* 47 (2009) 2436–2441.
- [6] L. Ke, R.S. Kumar, S.J. Chua, A.P. Burden, Degradation study in flexible substrate organic light-emitting diodes, *Appl. Phys. A* 81 (2005) 969–974.
- [7] Y. Letierrier, L. Medico, F. Demarco, J.A.E. Manson, U. Betz, M.F. Escola, M.K. Olsson, F. Atamny, Mechanical integrity of transparent conductive oxide films for flexible polymer-based displays, *Thin Solid Films* 460 (2004) 156–166.
- [8] V. Barone, J.E. Peralta, J. Uddin, G.E. Scuseria, Screened exchange hybrid density-functional study of the work function of pristine and doped single-walled carbon nanotubes, *J. Chem. Phys.* 124 (2006) 024709.
- [9] C.C. Wu, C.I. Wu, J.C. Sturm, A. Kahn, Surface modification of indium tin oxide by plasma treatment: An effective method to improve the efficiency, brightness, and reliability of organic light emitting devices, *Appl. Phys. Lett.* 70 (1997) 1348–1350.
- [10] Z.C. Wu, Z.H. Chen, X. Du, J.M. Logan, J. Sippel, M. Nikolou, K. Kamaras, J.R. Reynolds, D.B. Tanner, A.F. Hebard, A.G. Rinzler, Transparent, conductive carbon nanotube films, *Science* 305 (2004) 1273–1276.
- [11] Y.X. Zhou, L.B. Hu, G. Gruner, A method of printing carbon nanotube thin films, *Appl. Phys. Lett.* 88 (2006) 123109.
- [12] S. Kim, J. Yim, X. Wang, D.D.C. Bradley, S. Lee, J.C. Demello, Spin- and spray-deposited single-walled carbon-nanotube electrodes for organic solar cells, *Adv. Funct. Mater.* 20 (2010) 2310–2316.
- [13] D.H. Zhang, K. Ryu, X.L. Liu, E. Polikarpov, J. Ly, M.E. Tompson, C.W. Zhou, Transparent, conductive, and flexible carbon nanotube films and their application in organic light-emitting diodes, *Nano Lett.* 6 (2006) 1880–1886.
- [14] J. Li, L. Hu, L. Wang, Y. Zhou, G. Gruner, T.J. Marks, *Nano Lett.* 6 (2006) 2472–2477.
- [15] C.M. Aguirre, S. Auvray, S. Pigeon, R. Izquierdo, P. Desjardins, R. Martel, Carbon nanotube sheets as electrodes in organic light-emitting diodes, *Appl. Phys. Lett.* 88 (2006) 183104.
- [16] R. Krishnamoorti, K. Yurekli, C.A. Mitchell, Small-angle neutron scattering from surfactant-assisted aqueous dispersions of carbon nanotubes, *J. Am. Chem. Soc.* 126 (2004) 9902–9903.
- [17] R.E. Smalley, M.J. O'Connell, P. Boul, L.M. Ericson, C. Huffman, Y.H. Wang, E. Haroz, C. Kuper, J. Tour, K.D. Ausman, Reversible water-solubilization of single-walled carbon nanotubes by polymer wrapping, *Chem. Phys. Lett.* 342 (2001) 265–271.
- [18] D.E. Resasco, O. Matarredona, H. Rhoads, Z.R. Li, J.H. Harwell, L. Balzano, Dispersion of single-walled carbon nanotubes in aqueous solutions of the anionic surfactant NaDDBS, *J. Phys. Chem. B* 107 (2003) 13357–13367.
- [19] R.C. Haddon, H. Hu, B. Zhao, M.E. Itkis, Nitric acid purification of single-walled carbon nanotubes, *J. Phys. Chem. B* 107 (2003) 13838–13842.
- [20] M. Zhang, M. Yudasaka, S. Iijima, Diameter enlargement of single-wall carbon nanotubes by oxidation, *J. Phys. Chem. B* 108 (2004) 149–153.
- [21] R.E. Smalley, K.J. Ziegler, Z.N. Gu, H.Q. Peng, E.L. Flor, R.H. Hauge, Controlled oxidative cutting of single-walled carbon nanotubes, *J. Am. Chem. Soc.* 127 (2005) 1541–1547.
- [22] P. Vacca, G. Nenna, R. Miscioscia, D. Palumbo, C. Minarini, D. Della Sala, Patterned organic and inorganic composites for electronic applications, *J. Phys. Chem. C* 113 (2009) 5777–5783.
- [23] X.M. Tao, G.F. Wang, R.X. Wang, Flexible organic light-emitting diodes with a polymeric nanocomposite anode, *Nanotechnology* 19 (2008) 145201.
- [24] G. Gruner, E.C.W. Ou, L.B. Hu, G.C.R. Raymond, O.K. Soo, J.S. Pan, Z. Zheng, Y. Park, D. Hecht, G. Irvin, P. Drzica, Surface-modified nanotube anodes for high performance organic light-emitting diode, *ACS Nano* 3 (2009) 2258–2264.
- [25] T.J. Marks, J. Cui, A. Wang, N.L. Edleman, J. Ni, P. Lee, N.R. Armstrong, Indium tin oxide alternatives – High work function transparent conducting oxides as anodes for organic light-emitting diodes, *Adv. Mater.* 13 (2001) 1476.
- [26] C. Schrage, S. Kaskel, Flexible and transparent SWCNT electrodes for alternating current electroluminescence devices, *ACS Appl. Mater. Interfaces* 1 (2009) 1640–1644.
- [27] A. Southard, V. Sangwan, J. Cheng, E.D. Williams, M.S. Fuhrer, Solution-processed single walled carbon nanotube electrodes for organic thin-film transistors, *Org. Electron* 10 (2009) 1556–1561.
- [28] Y.M. Chien, F. Lefevre, I. Shih, R. Izquierdo, A solution processed top emission OLED with transparent carbon nanotube electrodes, *Nanotechnology* 21 (2010) 134020.
- [29] S. De, P.E. Lyons, S. Sorel, E.M. Doherty, P.J. King, W.J. Blau, P.N. Nirmalraj, J.J. Boland, V. Scardaci, J. Joimel, J.N. Coleman, Transparent, flexible, and highly conductive thin films based on polymer – nanotube composites, *ACS Nano* 3 (2009) 714–720.
- [30] H. Yan, P. Lee, N.R. Armstrong, A. Graham, G.A. Evmenenko, P. Dutta, T.J. Marks, High-performance hole-transport layers for polymer light-emitting diodes. Implementation of organosiloxane cross-linking chemistry in polymeric electroluminescent devices, *J. Am. Chem. Soc.* 127 (2005) 3172–3183.
- [31] L.B. Hu, J.F. Li, J. Liu, G. Gruner, T. Marks, Flexible organic light-emitting diodes with transparent carbon nanotube electrodes: problems and solutions, *Nanotechnology* 21 (2010) 55202.
- [32] B.T. Sullivan, J.A. Dobrowolski, R.C. Bajcar, optical interference, optical interference, contrast-enhanced electroluminescent device, *Appl. Optics* 31 (1992) 5988–5996.
- [33] L.S. Hung, J. Madathil, Reduction of ambient light reflection in organic light-emitting diodes, *Adv. Mater.* 13 (2001) 1787–1790.
- [34] Z.Y. Xie, L.S. Hung, High-contrast organic light-emitting diodes, *Appl. Phys. Lett.* 84 (2004) 1207.
- [35] J.-F. Li, S.-H. Su, K.-S. Hwang, M. Yokoyama, Enhancing the contrast and power efficiency of organic light-emitting diodes using CuPc/TiOPc as an anti-reflection layer, *J. Phys. D Appl. Phys.* 40 (2007) 2435–2439.
- [36] L.W. Zhaoxin Wu, Yong Qiu, Contrast-enhancement in organic light-emitting diodes, *Opt. Express* 13 (2005) 1406–1411.